Published OnlineFirst September 17, 2020; DOI: 10.1158/1535-7163.MCT-20-0030

Enhanced Immunotherapy with LHRH-R Targeted Lytic Peptide in Ovarian Cancer

Mark Seungwook Kim[1], Shaolin Ma[1,2], Anca Chelariu-Raicu[1,3], Carola Leuschner[4], Hector W. Alila[4], Sanghoon Lee[5], Robert L. Coleman[1], and Anil K. Sood[1,6,7]

ABSTRACT

Here, we examined the role of EP-100 [luteinizing hormone-releasing hormone (LHRH) ligand joined to a lytic peptide], improving the efficacy of immune checkpoint blockade. LHRH-R–positive murine ovarian cancer cells (ID8, IG10, IF5, and 2C12) were sensitive to EP-100 and were specifically killed at low micromolar levels through LHRH-R. EP-100 increased PD-L1 levels on murine ovarian cancer cells. *In vivo* syngeneic mouse models (ID8 and IG10) demonstrated that single-agent EP-100 reduced tumor volume, tumor weight, and ascites volume. The greatest reductions in tumor and ascites volume were observed with the combination of EP-100 with an anti–PD-L1 antibody. Immune profiling analysis showed that the population of $CD8^+$ T cells, natural killer cells, dendritic cells, and macrophages were significantly increased in tumor and ascitic fluid samples treated with anti–PD-L1, EP-100, and the combination. However, monocytic myeloid suppressor cells, B cells, and regulatory T cells were decreased in tumors treated with anti–PD-L1, EP-100, or the combination. *In vitro* cytokine arrays revealed that EP-100 induced IL1α, IL33, CCL20, VEGF, and Low-density lipoprotein receptor (LDLR) secretion. Of these, we validated increasing IL33 levels following EP-100 treatment *in vitro* and *in vivo*; we determined the specific biological role of $CD8^+$ T-cell activation with *IL33* gene silencing using siRNA and Cas9-CRISPR approaches. In addition, we found that $CD8^+$ T cells expressed very low level of LHRH-R and were not affected by EP-100. Taken together, EP-100 treatment had a substantial antitumor efficacy, particularly in combination with an anti–PD-L1 antibody. These results warrant further clinical development of this combination.

Introduction

Although immune checkpoint inhibitor therapies have revolutionized the treatment of some cancers (melanoma and lung), emerging clinical data show limited clinical efficacy of these agents in ovarian cancer, with objective response rates of 10% to 15%. It has been reported that infiltration of treatment-naïve tumors by T cells was associated with significantly prolonged median progression-free and overall survival compared with tumors with no T-cell infiltration(1, 2), and the high expression of PD-L1 on ovarian cancer cells was associated with poor outcome (3). Given the limited efficacy of immune therapy in ovarian cancer, there is a need for novel therapeutic strategies.

Among the many options for targeted therapy in ovarian cancer, we and others have considered the luteinizing hormone-releasing hormone receptor (LHRH-R) for selective delivery of drugs. LHRH-R is composed of 328 amino acids and is part of the rhodopsin-like G-protein–coupled receptor family (4, 5). LHRH-R is expressed at high levels in many tumor types, including prostate (6), breast (7), ovarian (8), endometrial (9), pancreatic (10), bladder (11), colorectal (12), hepatic (13) and renal cancers (14), melanoma (15), uveal melanoma (16), and non-Hodgkin lymphoma (17). Malignant cells typically display high expression of LHRH-R relative to their normal counterparts, except for the anterior pituitary basophil cells (18, 19). These findings support the concept that LHRH-R is not only a diagnostic marker in these cancers but also a potential molecular target for ovarian cancer therapy.

Therapeutic peptides have been used in the treatment of cancer; the benefits of using lytic peptide–based therapeutic agents include their small size and rapid cell lysing effects (20). The main limitation of lytic peptide–based reagents is their nonspecific cytotoxicity if untargeted and their immunogenicity. EP-100 is a synthetic 28-amino-acid fusion peptide consisting of the LHRH ligand joined without a linker to an 18-amino-acid cationic α-helical lytic peptide (CLIP-71) that targets LHRH-R (18). EP-100 induces cell membrane lysis rapidly via specific binding to cell surface LHRH-R in several human cancer cell lines (20, 21). A phase I study demonstrated that EP-100 was safe and well-tolerated, did not produce antidrug antibodies, and was not hemolytic. Although the MTD was not reached in the phase I study, treatment with EP-100 produced disease stabilization in 9 of 27 RECIST-evaluable advanced cancer patients (18). Based on the mechanism of action of EP-100 having direct lytic effects on the tumor cell membrane and killing cancer cells through necrosis, presenting tumor-associated antigens, we hypothesized that EP-100 would combine well with immune therapies and would increase the antitumor efficacy of an immune-stimulating agent in a synergistic manner. To test this hypothesis, we evaluated the therapeutic effect of EP-100 in combination with a checkpoint inhibitor in orthotopic, syngeneic murine ovarian cancer models. We found that EP-100 rapidly disrupted cell membranes via specific binding to cell surface

[1]Department of Gynecologic Oncology and Reproductive Medicine, The University of Texas MD Anderson Cancer Center, Houston, Texas. [2]Reproductive Medicine Research Center, the Sixth Affiliated Hospital of Sun Yat-Sen University, Guangzhou, China. [3]Department of Obstetrics and Gynecology, University of Hospital, LMU Munich, Germany. [4]Esperance Pharmaceuticals, Inc., Houston, Texas. [5]Department of System Biology, The University of Texas MD Anderson Cancer Center, Houston, Texas. [6]Department of Cancer Biology, The University of Texas MD Anderson Cancer Center, Houston, Texas. [7]Center for RNA Interference and Non-Coding RNA, The University of Texas MD Anderson Cancer Center, Houston, Texas.

Note: Supplementary data for this article are available at Molecular Cancer Therapeutics Online (http://mct.aacrjournals.org/).

Corresponding Authors: Mark Seungwook Kim, The University of Texas MD Anderson Cancer Center, 1881 East Road, 3SCR3 3642, Houston, TX 77054. Phone: 713-745-1304; Fax: 713-792-3643; E-mail: mkim3@mdanderson.org; and Anil K. Sood, Phone: 713-745-5266; E-mail: asood@mdanderson.org

Mol Cancer Ther 2020;19:2396–406

doi: 10.1158/1535-7163.MCT-20-0030

Published OnlineFirst September 17, 2020; DOI: 10.1158/1535-7163.MCT-20-0030

LHRH-R and induced a local immune response in combination with an anti–PD-L1 antibody. Together, these findings provide new insights into the potential for this membrane-specific lytic peptide in boosting immune response, an approach that may be applied in future immunotherapy.

Materials and Methods

Synthetic lytic peptide (EP-100)

Esperance Pharmaceuticals provided EP-100 (Chemical structure and amino acid sequences are in Supplementary Materials). The EP-100 drug substance was synthesized at American Peptide Company (now Bachem) following standard sFmoc [Nα-(9-Fluorenylmethoxycarbonyl)] solid-phase chemistry methods and is purified by standard reverse-phase high-performance liquid chromatography.

Cell lines and culture conditions

The murine ovarian cancer cell lines ID8, IG10, IF5, 2C12, and 3B11 were used for *in vitro* experiments; all were obtained from and authenticated by the Characterized Cell Line Core Facility at The University of Texas MD Anderson Cancer Center. The human ovarian cancer (SKOV3ip1) and murine immortalized fibroblast (NIH-3T3) and human $CD8^+$ cytotoxic T cells (ATCC PCS-800–017) were obtained from the American Type Culture Collection. Unless indicated otherwise, all *in vitro* experiments were performed with cell lines at 80% to 90% confluence. The cells were maintained in DMEM containing 10% FBS, 1 × insulin-transferrin-selenium (Thermo Fisher Scientific), and 0.5% gentamycin. The cells were free of pathogenic murine viruses and Mycoplasma (assayed by the PCR Mycoplasma Detection kit; cat #409010, MD Bioproducts). All cell lines were cultured at 37°C in an incubator with a 5% CO_2 atmosphere.

Western blot analysis

Briefly, whole-cell lysates were prepared by subjecting cells to lysis buffer [10 mmol/L Tris (pH 8.0), 1 mmol/L EDTA, 0.1% sodium dodecyl sulfate, 1% deoxycholate, 1% NP40, and 0.15 mol/L NaCl] containing a protease inhibitor mixture (Roche), and total proteins in 30-μg aliquots were isolated by using a BCA protein assay reagent kit (Pierce Biotechnology). Equal amounts of isolated proteins were separated by electrophoresis on 4% to 12% NuPAGE gels (Thermo Fisher Scientific) and transferred to nitrocellulose membranes. After blocking with Tris-buffered saline solution with 0.1% Tween20 containing 5% nonfat milk, the membranes were incubated with primary antibodies (1:1,000) at 4°C overnight. Blots were then exposed to horseradish peroxidase–conjugated secondary antibody (1:3,000) and visualized by the enhanced chemiluminescence detection kit (Pierce Biotechnology). To confirm equal protein loading, β-actin (0.1 μg/mL; Sigma-Aldrich) was used as a loading control.

Subcellular fractionation analysis

The subcellular protein fractionation kit (Thermo Fisher Scientific) was used to isolate LHRH-R and was isolated from the nuclear, cytoplasmic, and membrane proteins by using a subcellular protein fractionation kit (Thermo Fisher Scientific). The concentrations of the protein were determined using a BCA protein assay kit. Each nuclear, cytoplasmic, and membrane fraction was analyzed by Western blot.

Cytokine array

Supernatants from control and EP-100–treated ID8 cells were collected at 0, 2, 4, and 12 hours. Equal volumes (5 mL) of each culture supernatant were incubated with the precoated Proteome Profiler array membrane array (Proteome Profiler Mouse XL Cytokine Array kit; cat #ARY028, R&D Systems) and processed according to the manufacturer's protocol. Protein detection antibodies bound to the capture antibody were detected by streptavidin–horseradish peroxidase visualized by an enhanced chemiluminescence detection kit. Densitometric analysis of the dot blots was performed using Image J software.

IL33 ELISA

IL33 protein level in the supernatant (collected from ID8 cells treated with either EP-100 or PD-L1 antibody) was quantified by enzyme-linked immunosorbent assay (IL33 ELISA kit; Thermo Fisher Scientific) according to the manufacturer's protocol. IL33 was quantified using a standard curve derived from the manufacturer's IL33 standard. Experiments were done in triplicate.

Apoptosis assays

The percentages of apoptotic cells after treatment with EP-100 for 24 hours were determined by using an Annexin V–coupled FITC apoptosis detection kit-1 (BD Pharmingen) according to the manufacturer's protocol.

Quantitative RT-PCR analysis

Total RNA (1 μg/sample) was extracted from cells using an RNeasy Mini kit (Qiagen) and subjected to reverse transcription using a High-Capacity cDNA Reverse Transcription Kit (Applied Biosystems) according to the manufacturer's protocol. The cDNA synthesized was then used as the template in the quantitative PCR using specific TaqMan gene expression probes. Real-time amplification was performed on a 7900HT Fast system (Applied Biosystems), and endogenous control GAPDH expression level was calculated from the delta Ct values for the LHRH-R gene (22).

RNA interference

A siRNA against LHRH-R was purchased from Sigma-Aldrich (sequences are listed in Supplementary Table S1). A siRNA with the nonspecific function that shared no sequence homology with any known mRNA in a BLAST search was used as a control for target siRNA. Briefly, cancer cells at 50% to 60% confluency were transfected with a final concentration of 100 nmol/L of LHRH-R siRNA or the control siRNA. The knockdown of LHRH-R proteins was confirmed by RT-PCR and Western blot analysis after transfection for 48 hours or 72 hours. To determine the cytotoxicity of the EP-100 and anti–PD-L1 antibody combination, the cells were transfected with siRNA, then EP-100 and anti–PD-L1 antibody were added 24 hours after transfection. Cell viability was determined after 96 hours using the MTT assay.

Murine ovarian cancer model

All mouse studies were reviewed and approved by the Institutional Animal Care and Use Committee of MD Anderson Cancer Center. Female C57BL/6 mice (8 to 12 weeks old) were purchased from Taconic Biosciences. Each mouse received an i.p. injection of ID8 or IG10 (1×10^6 cells/0.2 mL of HBSS) to generate orthotopic models of ovarian cancer as described elsewhere (23). For each experiment, 10 mice in each group were used. After cancer cell injection, mice were randomly divided into four treatment groups: untreated control, single-agent anti–PD-L1 antibody (0.8 mg/kg intraperitoneally twice a week), single-agent EP-100 (0.2 mg/kg intravenously twice a week), or combined EP-100 plus anti–PD-L1 antibody at the same doses as the single-agent groups. Treatment was initiated 7 days after cancer

Published OnlineFirst September 17, 2020; DOI: 10.1158/1535-7163.MCT-20-0030

cell injection. To monitor tumor growth and response to treatment, mice were subjected to bioluminescence imaging and data acquisition on the first day of treatment and once a week afterward with the IVIS 100 imaging system coupled to the Living Image Software (Xenogen) as reported previously (24). Four weeks after tumor cell implantation, the mice were killed and their total body weight, tumor weight, number of tumor nodules, and ascites volume were recorded. The tumor specimens were carefully fixed in formalin, frozen in optimal cutting temperature medium, or snap-frozen for lysate preparation.

Cell viability assay

Cell viability was measured using MTT solution (Thermo Fisher Scientific) dissolved in PBS. Briefly, cells were seeded in a 96-well plate (3×10^3/well) and allowed to grow for 24 hours before treatment. Thereafter, the EP-100 was added to the culture medium at increasing doses for 72 hours. At the final time-point, cells were incubated with 0.5% MTT for 2 hours at 37°C. The supernatant was then discarded, the MTT formazan was dissolved in dimethyl sulfoxide (150 μL), and the absorbance was read at an optical density of 570 nm.

Immunofluorescence staining

The cultured cells were fixed for 10 minutes with 4% paraformaldehyde and blocked with 3% FBS and 1% BSA buffer for 1 hour at room temperature. After blocking, cells were incubated with anti–LHRH-R antibody (1:200; Origene Technologies) at 4°C overnight. After washing with PBS 3 times, cells were incubated with Alexa 488–labeled secondary antibodies (1:250 in blocking buffer; Jackson ImmunoResearch Laboratories) as recommended by the manufacturer. For nuclear staining, Hoechst 33258 dye was used (1:10,000; Invitrogen, Thermo Fisher Scientific). ProLong Diamond Antifade Mountant (Thermo Fisher Scientific) was then used to mount the stained cells on slides, which were covered with new, clean coverslips. The fluorescence signal on LHRH-R was imaged under a BZ9000 fluorescence microscope (Keyence) and analyzed by using Leica software.

Immune profiling assay

Immunophenotypes of single-cell suspensions from tumors were assessed by FACS flow cytometry. To stain myeloid-derived suppressor cells (MDSC), antibodies used were CD11b-APC (clone M1/70), Ly6G- FITC (clone 1A8), and Ly6C-PE (clone AL-21; all, BD Biosciences). For T-cell activation markers, cells were stained with an antibody specific for CD4-PE-Cy7 (clone RM4–5), CD8-PE-Cy7 (clone 53–6.7), CD62L-PE (clone MEL-14; all three, BD Biosciences), or CD44-FITC (clone IM7; Biolegend). After incubation on ice for 30 minutes, cells were washed and then fixed in PBS containing 1% formalin for analysis on an LSRII flow cytometer (BD Biosciences).

Statistical analysis

All quantitative data were analyzed and compared using the Prism software 8.0 (GraphPad Software). Statistical differences between each

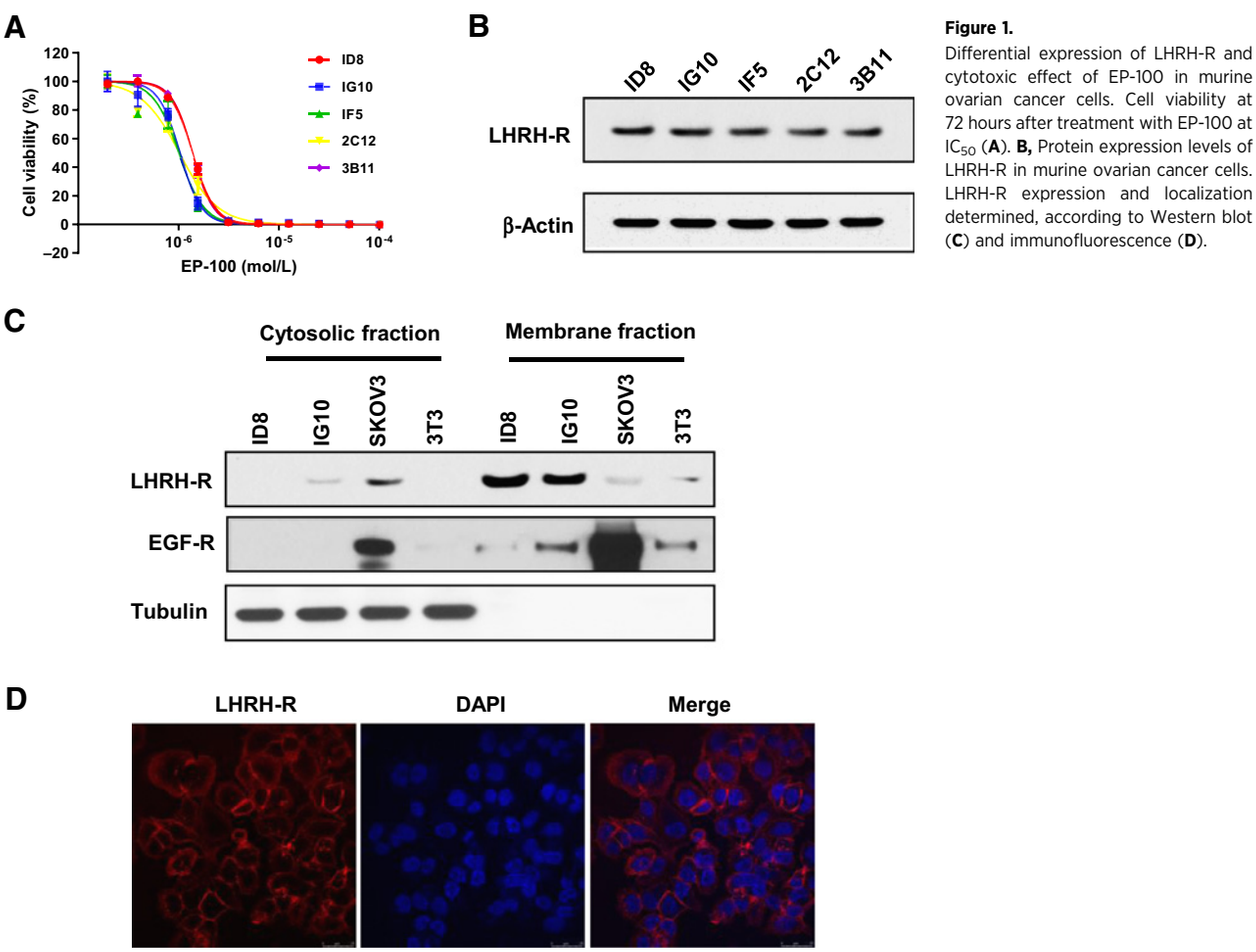

Figure 1.
Differential expression of LHRH-R and cytotoxic effect of EP-100 in murine ovarian cancer cells. Cell viability at 72 hours after treatment with EP-100 at IC_{50} (**A**). **B,** Protein expression levels of LHRH-R in murine ovarian cancer cells. LHRH-R expression and localization determined, according to Western blot (**C**) and immunofluorescence (**D**).

group were analyzed by the Student *t* test, and a *P* value less than 0.05 was considered statistically significant. All statistical tests were two-sided unless otherwise noted. Each experiment was performed at least 3 times.

Results

Expression of LHRH-R and cytotoxic effect of EP-100 in murine ovarian cancer cells

To identify the direct effects of EP-100 on cancer cells, we used murine ovarian cancer cell lines for *in vitro* experiments. The IC_{50} of EP-100 in these cell lines ranged from 1.0 to 1.3 μmol/L after 72 hours of treatment (**Fig. 1A**). We then measured the level of expression of LHRH-R in murine ovarian cancer cells using Western blot analysis. As shown in **Fig. 1B**, the protein level of LHRH-R was highly expressed in ID8, IG10, IF5, 2C12, and 3B11 cells. Because previous studies suggested that LHRH-R is expressed mainly on the cell membrane (1), we performed cell fractionation and immunofluorescence analyses. Indeed, LHRH-R was expressed mainly on the membrane of cancer cells (**Fig. 1C** and **D**). Human SKOV3ip1 ovarian cancer cells and immortalized murine 3T3 fibroblasts were used as negative controls.

To determine whether the antitumor EP-100 efficacy is specific to LHRH-R expression, we silenced LHRH-R using siRNA (**Fig. 2A**). As shown in **Fig. 2B** and **C**, cells in which LHRH-R was silenced remained viable after treatment with EP-100, whereas control cells treated with nonspecific siRNA were killed. In addition, treatment with untargeted lytic peptide, CLIP-71 lacking the LHRH ligand, or leuprolide acetate alone did not have cytotoxic effects (**Fig. 2D** and **E**). These data demonstrate that murine ovarian cancer cells were sensitive to EP-100 and were specifically killed at low micromolar levels through LHRH-R.

EP-100 combination with immune therapy

To determine the potential role of EP-100 in immune activation, we determined its effects on PD-L1 expression. As shown in **Fig. 3A** and **B**, both PD-L1 mRNA and protein levels were increased in ID8 and IG10 cells following treatment with EP-100. PD-L1 mRNA was increased with treatment with as low as 0.5 μmol/L EP-100 for 4 hours, and PD-L1 protein was increased after 6 hours of treatment. To determine the antitumor effects of EP-100 alone and in combination with the anti–PD-L1 antibody, we used the ID8 or IG10 syngeneic orthotopic ovarian cancer models. As shown in **Fig. 3C** and **D**, weekly bioluminescence images showed steady increases in the luminescence counts of tumors in the control group (from $9.2 \pm 1.2 \times 10^4$ to $180.5 \pm 24.3 \times 10^4$ at the end of the study), the single-agent anti–PD-L1 antibody group (from $9.2 \pm 1.2 \times 10^4$ to $118.7 \pm 28.7 \times 10^4$), and, at a lower rate, the single-agent EP-100 group (from $9.2 \pm 1.2 \times 10^4$ to $88.6 \pm 21.5 \times 10^4$). All values reported are mean ± SD unless otherwise indicated. The combined EP-100 plus anti–PD-L1 antibody delayed tumor growth through day 14, 1 week after treatment began, and the tumor increased from $9.2 \pm 1.2 \times 10^4$ to $30.7 \pm 4.3 \times 10^4$ ($P < 0.002$) at the end of the study. At the end of the experiment on day 28, the body weights of the host mice in all four groups were not affected (**Fig. 3E**). At necropsy, ascitic fluid was removed and measured, and tumors were removed and weighed. The effects of EP-100 and anti–PD-L1 antibody on primary tumor weight are shown in **Fig. 3F**. Tumor weights were significantly lower in all three treatment groups than in controls (1.06 ± 0.08 g): single-agent anti–PD-L1 antibody (0.54 ± 0.06 g, $P < 0.005$), single-agent EP-100 (0.49 ± 0.07 g, $P < 0.005$), and combined EP-100 plus anti–PD-L1 antibody (0.29 ± 0.03 g, $P < 0.001$ vs. control, $P < 0.01$ vs. single agents). Tumor growth was moderately inhibited by a single-agent anti–PD-L1 antibody (60.1%) and single-agent EP-100 (60.1%) and was inhibited to a greater degree by combining EP-100 plus anti–PD-L1 antibody (82.7%). Ascites volume was lower in all three treatment groups than in controls (12.26 ± 0.6 mL): it was 10.2 ± 0.6 mL in the single-agent anti–PD-L1 antibody group ($P < 0.01$) and 8.0 ± 0.7 mL in the single-agent EP-100 group ($P < 0.004$, **Fig. 3G**). The combination treatment resulted in the lowest volume of ascites, 5.6 ± 0.4 mL ($P < 0.0001$ vs. control, $P < 0.0006$ vs. both single agents). The relative reductions of ascites volume were 15% in the anti–PD-L1 antibody group and 35.5% in the EP-100 group. The greatest reduction was measured in the combination group (58.4%). Similar results were observed for combined EP-100 plus anti–PD-L1 antibody in the IG10 model. Tumor weights were lower in treatment groups than in controls (1.04 ± 0.2 g): anti–PD-L1 antibody (0.62 ± 0.17 g, $P < 0.05$), single-agent EP-100 (0.45 ± 0.2 g, $P < 0.01$), and combined EP-100 plus anti–PD-L1 antibody (0.26 ± 0.1 g, $P < 0.001$ vs. control, $P < 0.05$ vs. single agents). Ascites volumes were reduced in all three treatment groups, but the greatest reductions were in the combination treatment group (Supplementary Fig. S1).

Combined EP-100 and PD-L1 blockade increased antitumor effector T cells *in vivo*

To determine the effect of EP-100 on tumor microenvironment, we analyzed the immune cell profiles in tumors and ascitic fluid in each treatment group using FACS. As shown in **Fig. 4A**, the $CD45^+$ cell fraction in all live cells was 8.16% ± 1.3% in tumors from control mice, 12.83% ± 1.1% in tumors from mice treated with single-agent anti–PD-L1 antibody ($P = 0.75$ vs. controls), 26.1% ± 5.2% in tumors from mice treated with single-agent EP-100 ($P < 0.03$ vs. controls), and 22.5% ± 5.8% in the tumors from mice treated with combined EP-100 plus anti–PD-L1 antibody ($P = 0.08$ vs. controls). The subpopulation of $CD8^+$ T cells as a percentage of $CD45^+$ cells was significantly greater in tumors from mice treated with anti–PD-L1 antibody (10.7% ± 0.8%, $P < 0.003$ vs. controls), EP-100 (15.5% ± 0.8%, $P < 0.0001$ vs. controls), or the combination (14.7% ± 1.7%, $P < 0.0002$ vs. controls, $P < 0.01$ vs. single-agent EP-100) than in tumors from control mice (2.6% ± 0.4%). The percentage of regulatory T cells (Treg) was highest in control tumors (1.14% ± 0.09%), similar in tumors from mice treated with anti–PD-L1 antibody (0.91% ± 0.13%, $P = 0.41$ vs. controls) or EP-100 (0.95% ± 0.15%, $P = 0.53$ vs. controls), and lowest in tumors from mice treated with the combination (0.23% ± 0.01%, $P < 0.0012$ vs. controls; $P < 0.005$ vs. EP-100). Natural killer (NK) cells made up 3.76% ± 0.13% of $CD45^+$ cells in tumors from control mice; these percentages were greater in tumors of mice treated with anti–PD-L1 antibody (8.16% ± 0.31%, $P = 0.066$ vs. controls), EP-100 (10.67% ± 1.4%, $P < 0.0075$ vs. controls), and to the greatest extent in those of mice treated with combined EP-100 plus anti–PD-L1 antibody (14.27% ± 1.8%, $P < 0.005$ vs. controls). Macrophages made up 1.6% ± 0.05% of $CD45^+$ cells in tumors from controls; these percentages were greater in tumors of mice treated with anti–PD-L1 antibody (6.64% ± 0.2 %, $P < 0.001$ vs. controls), EP-100 (10.1% ± 0.13 %, $P < 0.0001$ vs. controls; $P < 0.01$ vs. anti–PD-L1 antibody), or the combination (11.36% ± 1.2%, $P < 0.0001$ vs. controls). The subpopulation of B cells as a percentage of $CD45^+$ cells was highest in tumors from control mice (12.14% ± 0.9%), but this percentage was not significantly different than those in tumors from mice treated with anti–PD-L1 antibody (10.9% ± 0.16%, $P = 0.87$ vs. controls), EP-100 (10.1% ± 2.4%, $P = 0.61$ vs. controls), or EP-100 plus anti–PD-L1 antibody (7.3% ± 0.76%, $P = 0.09$ vs. controls). The subpopulation of dendritic cells as a percentage of $CD45^+$ cells was higher in tumors from all three treatment groups than in tumors from controls (1.88% ± 0.03%):

Published OnlineFirst September 17, 2020; DOI: 10.1158/1535-7163.MCT-20-0030

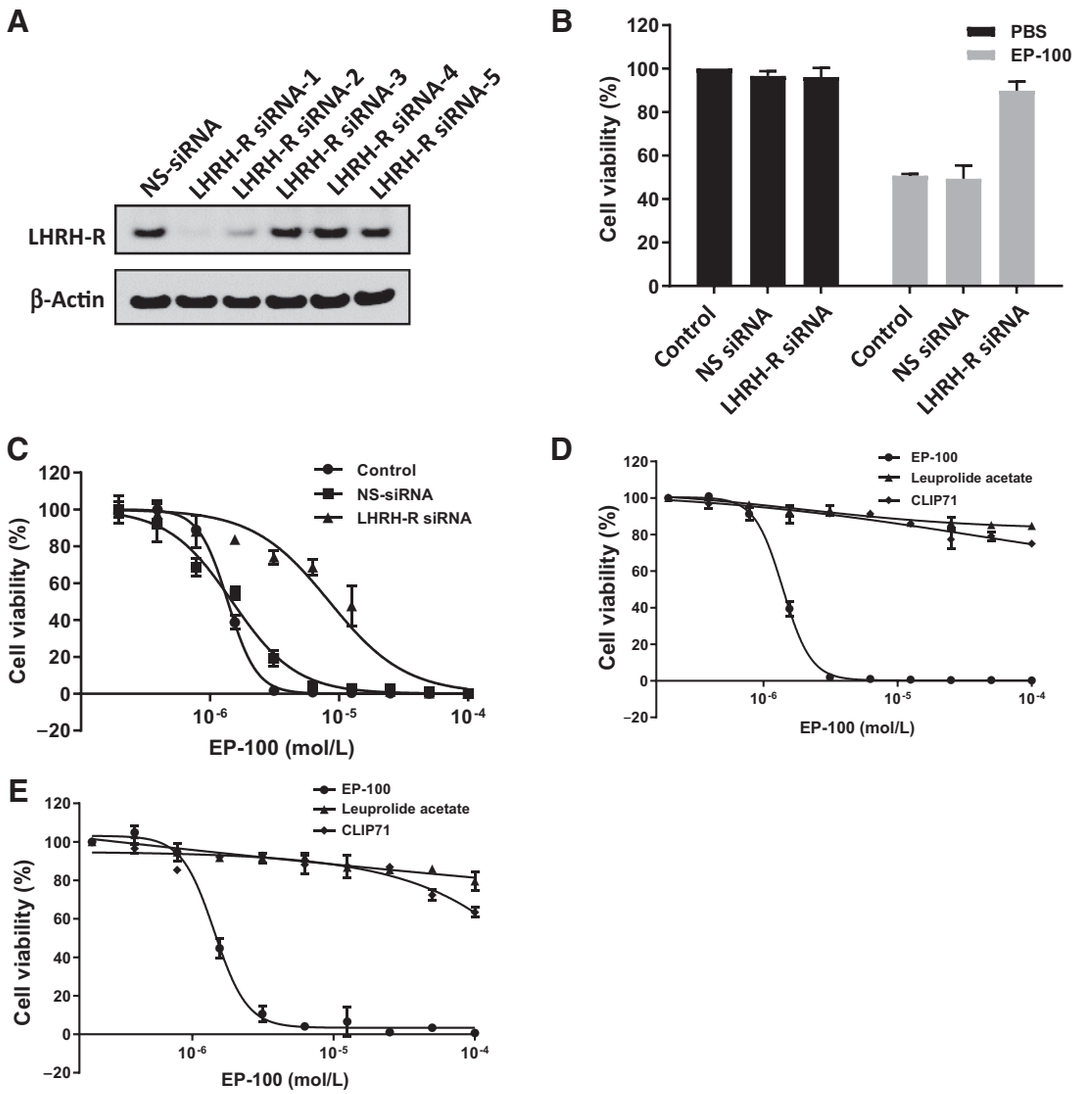

Figure 2.

LHRH-R is essential for EP-100–mediated cytotoxicity in cancer cells. ID8 cells were transfected with 100 nmol/L of various siRNAs targeting LHRH-R (**A**). Nonspecific siRNA (NS-siRNA) was used as control. **B,** Cell viability assay. siRNA targeting LHRH-R transfected to ID8 cell for 48 hours and then vehicle (PBS) or 1 μmol/L EP-100 further 24 hours, then cell viability was measured. **C,** MTT assay. ID8 cells were cultured with various concentrations of EP-100 for 72 hours, and then cell viability was measured. Cell viability of ID8 (**D**) and IG10 (**E**) cancer cells in the presence of various concentrations of EP-100, leuprolide acetate, or CLIP-71.

anti–PD-L1 antibody (3.01% ± 0.18%, $P < 0.009$ vs. controls), EP-100 (5.12% ± 0.34%, $P < 0.0001$ vs. controls), and combination treatment (5.43% ± 0.4%, $P < 0.0001$ vs. controls). The subpopulation of monocytic MDSCs (mMDSC) as a percentage of $CD45^+$ cells was lower in tumors from all three treatment groups than in controls (1.5% ± 0.006%): anti–PD-L1 antibody (1.01% ± 0.1%, $P < 0.015$ vs. controls), EP-100 (1.015% ± 0.15%, $P < 0.022$ vs. controls), and (to the greatest extent) combination treatment (0.38% ± 0.03%, $P < 0.0001$ vs. controls; $P < 0.002$ vs. anti–PD-L1 antibody). The ratio of $CD8^+$ T cells to Tregs was lowest in tumors from the control group (2.27 ± 0.26), higher in tumors treated with anti–PD-L1 antibody (11.01 ± 2.2, = 0.26 vs. controls), nearly 8 times higher in tumors treated with in EP-100 (15.5 ± 2.5, $P < 0.001$ vs. controls) and nearly 30 times higher in tumors treated with the combination (65.2 ± 1.4, $P < 0.0009$ vs. controls). The effects of these treatments on immune cells in ascitic fluid were similar (**Fig. 4B**). These data indicate that EP-100 promotes a tumor microenvironment that is favorable to tumor lysis as indicated by an increase of $CD8^+$ T cells, NK cells, dendritic cells, and macrophages while suppressing immune-inhibitory cells such as Tregs, B cells, and mMDSCs. These results show that the effects of combined treatment with EP-100 plus anti–PD-L1 antibody in reducing numbers of live tumor cells, tumor weights, and ascites could be driven by immune modulation through EP-100.

EP-100 induced increased IL33 expression in $CD8^+$ T cells

A proteome profiler murine cytokine array was used to analyze the effects of EP-100 on cytokine and chemokine secretion in the $CD8^+$ T-cell activation in ID8 ovarian cancer cells. To investigate

Published OnlineFirst September 17, 2020; DOI: 10.1158/1535-7163.MCT-20-0030

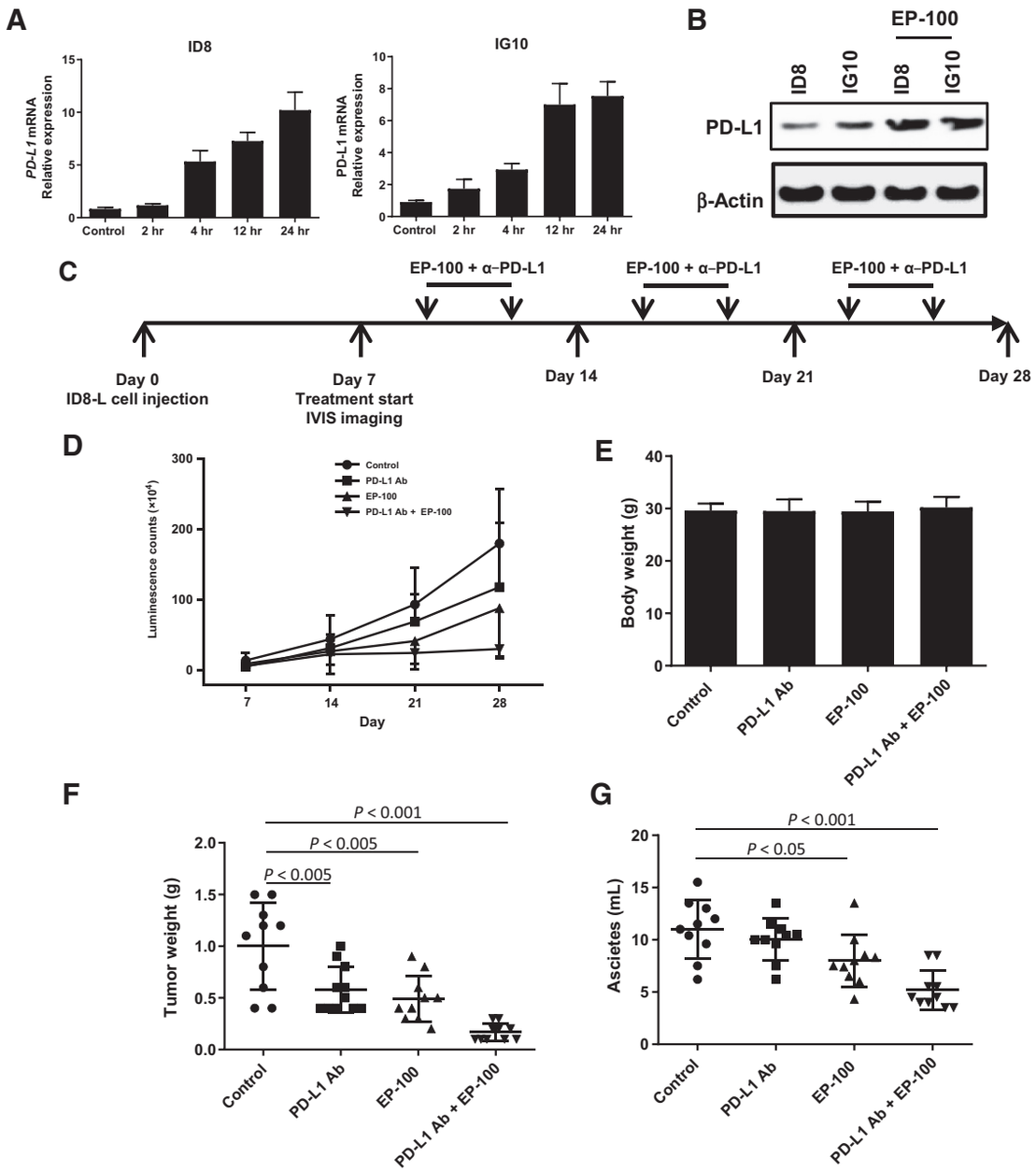

Figure 3.

EP-100 combination therapy with immune checkpoint blockade in ovarian cancer orthotopic xenograft models. ID8 and IG10 cells were cultured in the presence of EP-100 for the indicated periods, and *PD-L1* mRNA (**A**) and protein (**B**) expressions were determined. The schedule of treatment with combination EP-100 plus anti–PD-L1 antibody (**C**). The effect of this combination on the size of established tumors from mice injected with ID8-luciferase was evaluated by luminescence counts (**D**). Error bars, SD. Mice inoculated intraperitoneally with ID8-luciferase cells were treated with vehicle (control), single-agent anti–PD-L1 antibody (0.8 mg/kg intraperitoneally twice a week), EP-100 (0.2 mg/kg intravenously twice a week), or a combination of EP-100 plus anti–PD-L1 antibody. Effects on body weight (**E**), tumor growth (**F**), and ascites (**G**) are shown.

the cytokine and chemokine secretion in media, we collected the supernatants followed by treatment with 1 μmol/L EP-100 for 2, 4, and 12 hours and then analyzed these using the Proteome Profiler Mouse XL Cytokine Array Kit (R&D Systems). As shown in **Fig. 5A**, EP-100 increased secretion of various molecules, including leukemia-inhibitory factor (LIF), CXCL10, IL1α, CCL20, VEGF, IL33, and LDL receptor. Both LIF and CXCL10 secretion were decreased after treatment with EP-100 for 4 hours. LDL receptor secretion was increased by EP-100 at 2 and 12 hours, whereas IL1α, CCL20, VEGF, and IL33 were secreted after EP-100 treatment. Among the cytokines, we found that IL33 inhibits tumor growth and modifies the tumor microenvironment (25, 26). We validated EP-100–induced IL33 using RT-PCR and ELISA. IL33 mRNA expression was increased in 30 minutes after EP-100 treatment, and secretion was increased after 2 hours of EP-100

Published OnlineFirst September 17, 2020; DOI: 10.1158/1535-7163.MCT-20-0030

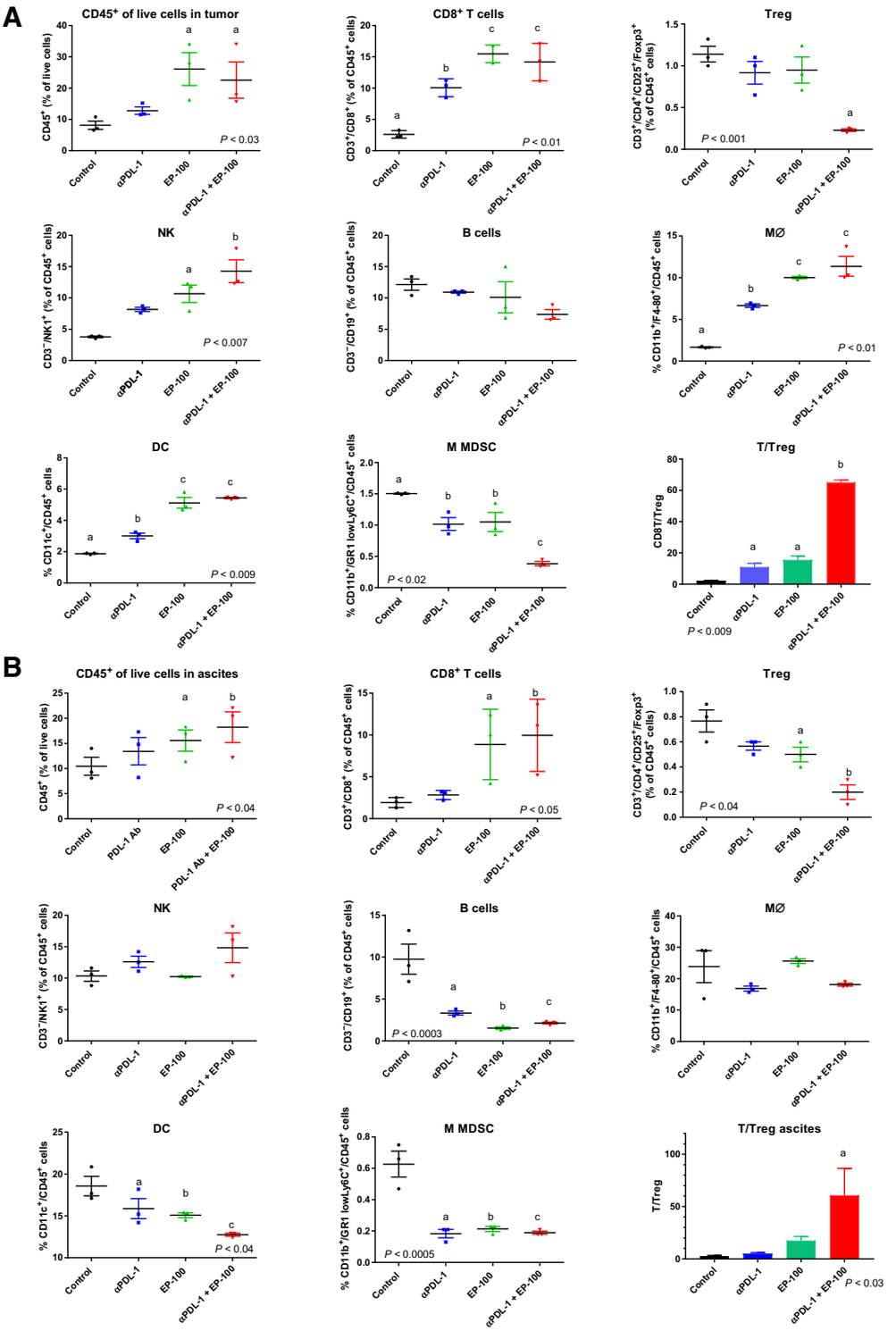

Figure 4.

Immune cell profiling of EP-100 combination therapy with immune checkpoint blockade in ovarian cancer orthotopic xenograft models. Immune profiles in the tumor (**A**) and ascitic fluid (**B**) were assessed using FACS flow cytometry with ID8-luciferase cancer cells. The $CD45^+$ cell fraction was isolated in the gate of live cells after dissociation of tumor tissues. $CD8^+$ T cells were defined as $CD45^+CD3^+CD4^-CD8^+$, Tregs as $CD45^+CD3^+CD4^+CD25^+FoxP3^+$, NK cells as $CD45^+$ NK1, B cells as $CD45^+/CD19^+$, macrophages as $CD45^+/CD11b^+/F4/80^+$, dendritic cells as $CD45^+/CD11b^+/CD11c$, and mMDSCs as $CD45^+CD3^-CD11b^+Ly6G^-Ly6C^{high}$. Each dot represents data from 1 mouse.

Published OnlineFirst September 17, 2020; DOI: 10.1158/1535-7163.MCT-20-0030

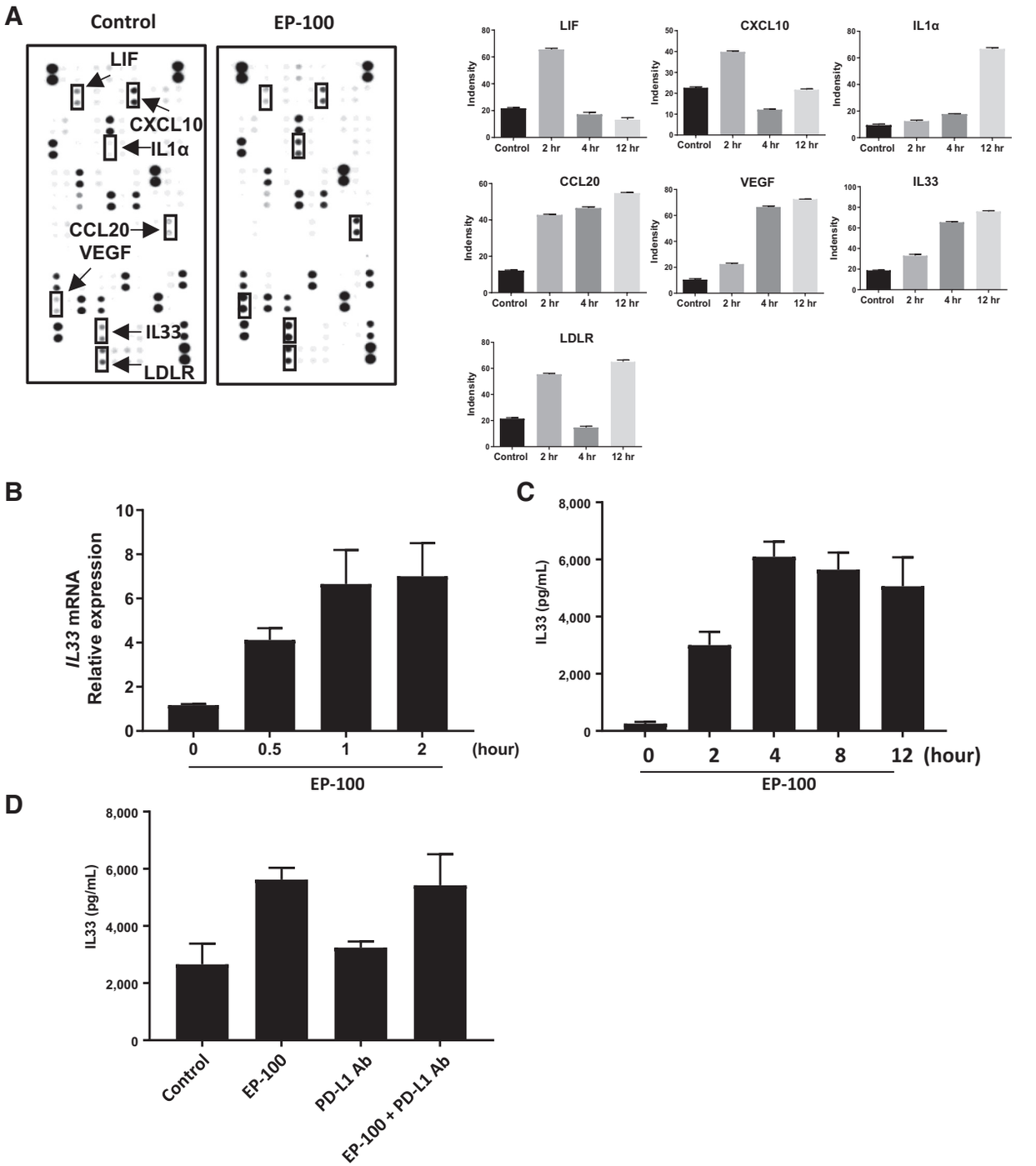

Figure 5.

Array analysis of cytokine and chemokine secretion by ID8 cells treated with EP-100 for 2, 4, and 12 hours. Array images show spots of each cytokine or chemokine detected from the cell culture medium of ID8 cells that were untreated (control) or treated with EP-100 for 12 hours (**A**). The densitometric analysis of the dot blots was measured using Image J software (**B**). **C** and **D,** mRNA expression and protein secretion of IL33 with EP-100 for various times in ID8 cells. **D,** Secretion of IL33 with single-agent EP-100, a single-agent PD-L1 antibody, or EP-100 combination with PD-L1 antibody treatment on ID8 cells.

treatment, and this effect continued through 12 hours (**Fig. 5B** and **C**). In addition, the PD-L1 antibody had no effect on IL33 secretion (**Fig. 5D**). To investigate the functional role of IL33 in the tumor microenvironment, we tested the IL33 effect on T-cell differentiation and activation *in vitro*. We first isolated naïve $CD4^+$ T cells from mouse spleen for the *in vitro* experiments. The isolated naïve $CD4^+$ T

Published OnlineFirst September 17, 2020; DOI: 10.1158/1535-7163.MCT-20-0030

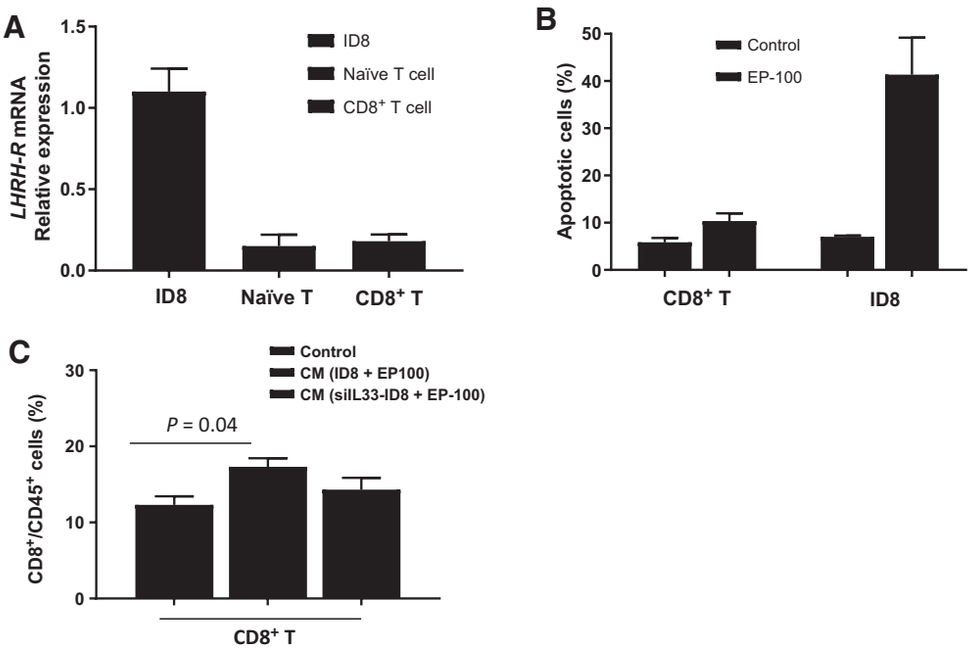

Figure 6.

Role of IL33 in T-cell activation. Naïve T cells were isolated from mouse spleen and then further cultured with complete media containing CD3 and CD28, and mouse IL2. *LHRH-R* expression level (**A**) and EP-100 cytotoxic effect (**B**) on naïve T cells and $CD8^+$ T cells. **C,** The naïve $CD4^+$ T cells from mouse spleen were cultured in CM from the EP-100–treated ID8 cells or CM from IL33 knockdown ID8 cells. CM from EP-100 nontreated ID8 cells was used as control. The $CD8^+$ T-cell population was measured by FACS.

cells differentiated $CD8^+$ T cells in complete media containing CD3 and CD28, and mouse IL2 for 5 days (27, 28). As shown in **Fig. 6A** and **B**, we found low expression level of LHRH-R in naïve $CD4^+$ T cells and $CD8^+$ T cells, and low cytotoxic effect of EP-100 on $CD8^+$ T cells. Next, we obtained EP-100–treated conditioned media (CM) from either ID8 cells or IL33 knockdown ID8 cells. As shown in **Fig. 6C**, we found that CM from EP-100–treated ID8 cells significantly increased the proportion of $CD8^+$ T cells compared with control CM (EP-100 nontreated CM from ID8 cells; 17.3 ± 1.1 vs. 12.3 ± 1.1, $P = 0.04$). However, CM from the EP-100–treated IL33 silenced ID8 cells did not increase the proportion of $CD8^+$ T cells (**Fig. 6C**). Next, to investigate the ability of IL33 to promote the migration of T cells, we utilized an *in vitro* transwell migration assay using human $CD8^+$ T cells. We found that CM from EP-100–treated ID8 cells increased T-cell migration compared with control CM. In contrast, CM from IL33 knockdown ID8 cells did not affect T-cell migration ability (Supplementary Fig. S2D). These results demonstrate that EP-100–induced IL33 promotes cytotoxic T-cell migration.

Discussion

In this study, we determined EP-100 can have both direct antitumor effects as well as functioning as an immune stimulant. We found that EP-100 rapidly disrupted the cell membrane via specific binding to cell surface LHRH-R, increased PD-L1 levels on tumor cells, and increased effects of PD-L1 checkpoint blockade. We observed, through a combination of EP-100 and anti–PD-L1 antibody therapy, that EP-100 induced anticancer activity and changed the tumor microenvironment in favor of tumor lysis by increasing the antitumor immune cell population while reducing immune-inhibitory populations. In addition, we found that EP-100–induced IL33 has an essential role in immune modulation through increasing cytotoxic T-cell population.

EP-100 highlights an emerging new class of anticancer drugs that have the advantage of acting rapidly through cell surface receptor–associated rapid membrane disruption in both drug-sensitive and drug-resistant tumors, independent of cancer cell proliferation. The cell surface receptor LHRH-R is overexpressed in many solid tumors and hematologic malignancies but is expressed at low levels in vital organs, except for the pituitary gland and the gonads (29). LHRH-R has been reported to be rapidly internalized and recycled, as demonstrated by the accumulation of compounds through receptor-mediated uptake (30, 31). EP-100 is designed to target and specifically kill cancer cells that overexpress LHRH-R via a novel mechanism that induces both direct membrane disruption and necrosis. Our *in vitro* studies demonstrated that the cytotoxic effect of EP-100 was associated with LHRH-R expression on the target cells, and EP-100′s high degree of specificity was determined by comparing it with a lytic peptide formed by fusing LHRH to CLIP-71.

In phase I clinical study, EP-100 was shown to be safe and well-tolerated, with no major organ toxicity. Likewise, the mice treated with EP-100 in our *in vivo* studies demonstrated no weight loss or behavioral changes, a finding consistent with the absence of side effects from EP-100 at a therapeutically effective dose (0.2 mg/kg). Compared with other lytic peptide conjugates now in preclinical studies, such as targeting peptide for PSMA, anti-CD33, HER2, and gastrin-leasing peptide receptor (32–36), EP-100 showed a much greater cytotoxic effect *in vitro* at low micromolar concentrations. EP-100 and other conjugates of CLIP-71 were highly active when administered systemically at low doses (0.2 mg/kg), killing cancer cells by necrosis rather than apoptosis (18, 21). Our *in vitro* and *in vivo* results demonstrate that EP-100

induced PD-L1 expression in cancer cells and immune modulation that favorably changed the tumor microenvironment toward increasing populations of immune cells that induce tumor lysis ($CD8^+$ T cells, NK cells, dendritic cells, and macrophages) while reducing immune-inhibitory populations (Tregs, B cells, and mMDSCs). Various immune cells, such as T cells, B cells, NK cells, and macrophages, are known to infiltrate tumors. $CD8^+$ T cells and NK cells are the most effective for establishing antitumor immunity (37, 38). Here, we discovered an important role for IL33 in this immunity. When induced by EP-100, IL33 increased the infiltration of $CD8^+$ T cells both *in vitro* and *in vivo*. Other investigators also have reported the antitumor effect of IL33 (25, 39). It appears that IL33 activates $CD8^+$ T cells and NK cells that can directly kill tumor cells. However, the precise molecular mechanisms connecting IL33 with tumor growth inhibition and immune surveillance are not fully understood.

The exact mechanism by which EP-100 induces its antitumor effects has not yet been resolved, and there are not yet biomarkers to predict and monitor which patients and tumors will show a response to this drug. Taken together, however, our findings demonstrate that EP-100 rapidly kills LHRH-R–expressing cancer cells at low micromolar levels that are achievable in humans. Our *in vivo* results show that EP-100 was highly active when administered as a short-term intravenous infusion, even though it has a limited half-life in the bloodstream. In conclusion, EP-100 may have clinical applications for multidrug-resistant ovarian cancers and other LHRH-R–positive cancers, such as breast, prostate, endometrial, pancreatic, uterine sarcoma, testicular, skin cancers (melanoma), liver, lung, and uveal melanoma as well as hematologic malignancies such as non-Hodgkin lymphoma and leukemia.

Disclosure of Potential Conflicts of Interest

H.W. Alila and C. Leuschner is an employee of Esperance Pharmaceuticals, the company that provided the drug and financial support for the study. R.L. Coleman reports grants from Esperance (funding for clinical trial), grants and personal fees from Merck (funding for clinical trial and SAB), grants and personal fees from AstraZeneca (funding for clinical trial and SAB), and grants and personal fees from GSK/Tesaro (funding for clinical trial and SAB) during the conduct of the study. A.K. Sood reports grants from Esperance (Research grant) during the conduct of the study; personal fees from Merck (Consulting), personal fees from Kiyatec (Consulting), grants from MTrap (Research funding), and other from BioPath (Shareholder) outside the submitted work. No potential conflicts of interest were disclosed by the other authors.

Authors' Contributions

M.S. Kim: Investigation, writing-original draft, project administration, writing-review and editing. **S. Ma:** Investigation, writing-review and editing. **A. Chelariu-Raicu:** Investigation. **C. Leuschner:** Conceptualization, data curation, project administration, writing-review and editing. **H.W. Alila:** Project administration, writing-review and editing. **S. Lee:** Validation, writing-review and editing. **R.L. Coleman:** Project administration, writing-review and editing. **A.K. Sood:** Conceptualization, resources, validation, investigation, project administration, writing-review and editing.

Acknowledgments

Editorial support was provided by Bryan Tutt in the Department of Scientific Publications, The University of MD Anderson Cancer Center, Houston, TX.

This work was supported by in part by other NIH grants (P30CA016672, CA213759, P50CA217685, P50CA098258, and R35CA209904), the Blanton-Davis Ovarian Cancer Research Program, the American Cancer Society Research Professor Award, and the Frank T. McGraw Memorial Chair in Cancer Research.

The costs of publication of this article were defrayed in part by the payment of page charges. This article must therefore be hereby marked *advertisement* in accordance with 18 U.S.C. Section 1734 solely to indicate this fact.

Received January 14, 2020; revised June 8, 2020; accepted August 26, 2020; published first September 17, 2020.

References

1. Szende B, Srkalovic G, Timar J, Mulchahey JJ, Neill JD, Lapis K, et al. Localization of receptors for luteinizing hormone-releasing hormone in pancreatic and mammary cancer cells. Proc Natl Acad Sci U S A 1991;88:4153–6.
2. Zhang L, Conejo-Garcia JR, Katsaros D, Gimotty PA, Massobrio M, Regnani G, et al. Intratumoral T cells, recurrence, and survival in epithelial ovarian cancer. N Engl J Med 2003;348:203–13.
3. Hamanishi J, Mandai M, Iwasaki M, Okazaki T, Tanaka Y, Yamaguchi K, et al. Programmed cell death 1 ligand 1 and tumor-infiltrating CD8+ T lymphocytes are prognostic factors of human ovarian cancer. Proc Natl Acad Sci U S A 2007;104:3360–5.
4. Neill JD, Musgrove LC, Duck LW. Newly recognized GnRH receptors: function and relative role. Trends Endocrinol Metab 2004;15:383–92.
5. Cheng CK, Leung PC. Molecular biology of gonadotropin-releasing hormone (GnRH)-I, GnRH-II, and their receptors in humans. Endocr Rev 2005;26:283–306.
6. Liu SV, Schally AV, Hawes D, Xiong S, Fazli L, Gleave M, et al. Expression of receptors for luteinizing hormone-releasing hormone (LH-RH) in prostate cancers following therapy with LH-RH agonists. Clin Cancer Res 2010;16:4675–80.
7. Schally AV, Nagy A. Chemotherapy targeted to cancers through tumoral hormone receptors. Trends Endocrinol Metab 2004;15:300–10.
8. Westphalen S, Kotulla G, Kaiser F, Krauss W, Werning G, Elsasser HP, et al. Receptor mediated antiproliferative effects of the cytotoxic LHRH agonist AN-152 in human ovarian and endometrial cancer cell lines. Int J Oncol 2000;17:1063–9.
9. Kovacs M, Schally AV. Comparison of mechanisms of action of luteinizing hormone- releasing hormone (LHRH) antagonist cetrorelix and LHRH agonist triptorelin on the gene expression of pituitary LHRH receptors in rats. Proc Natl Acad Sci U S A 2001;98:12197–202.
10. Szepeshazi K, Lapis K, Schally AV. Effect of combination treatment with analogs of luteinizing hormone-releasing hormone (LH-RH) or somatostatin and 5-fluorouracil on pancreatic cancer in hamsters. Int J Cancer 1991;49:260–6.
11. Szepeshazi K, Schally AV, Keller G, Block NL, Benten D, Halmos G, et al. Receptor-targeted therapy of human experimental urinary bladder cancers with cytotoxic LH-RH analog AN-152 [AEZS-108]. Oncotarget 2012;3:686–99.
12. Szepeshazi K, Schally AV, Halmos G. LH-RH receptors in human colorectal cancers: unexpected molecular targets for experimental therapy. Int J Oncol 2007;30:1485–92.
13. Hao D, Sun L, Hu X, Hao X. (99m)Tc-LHRH in tumor receptor imaging. Oncol Lett 2017;14:569–78.
14. Keller G, Schally AV, Gaiser T, Nagy A, Baker B, Halmos G, et al. Receptors for luteinizing hormone releasing hormone expressed on human renal cell carcinomas can be used for targeted chemotherapy with cytotoxic luteinizing hormone releasing hormone analogues. Clin Cancer Res 2005;11:5549–57.
15. Keller G, Schally AV, Gaiser T, Nagy A, Baker B, Westphal G, et al. Human malignant melanomas express receptors for luteinizing hormone releasing hormone allowing targeted therapy with cytotoxic luteinizing hormone releasing hormone analogue. Cancer Res 2005;65:5857–63.
16. Treszl A, Steiber Z, Schally AV, Block NL, Dezso B, Olah G, et al. Substantial expression of luteinizing hormone-releasing hormone (LHRH) receptor type I in human uveal melanoma. Oncotarget 2013;4:1721–8.
17. Keller G, Schally AV, Gaiser T, Nagy A, Baker B, Halmos G, et al. Receptors for luteinizing hormone releasing hormone (LHRH) expressed in human non-Hodgkin's lymphomas can be targeted for therapy with the cytotoxic LHRH analogue AN-207. Eur J Cancer 2005;41:2196–202.
18. Curtis KK, Sarantopoulos J, Northfelt DW, Weiss GJ, Barnhart KM, Whisnant JK, et al. Novel LHRH-receptor-targeted cytolytic peptide, EP-100: first-in-human phase I study in patients with advanced LHRH-receptor-expressing solid tumors. Cancer Chemother Pharmacol 2014;73:931–41.

Published OnlineFirst September 17, 2020; DOI: 10.1158/1535-7163.MCT-20-0030

19. Dharap SS, Wang Y, Chandna P, Khandare JJ, Qiu B, Gunaseelan S, et al. Tumor-specific targeting of an anticancer drug delivery system by LHRH peptide. Proc Natl Acad Sci U S A 2005;102:12962–7.
20. Leuschner C, Hansel W. Membrane disrupting lytic peptides for cancer treatments. Curr Pharm Des 2004;10:2299–310.
21. Ma S, Pradeep S, Villar-Prados A, Wen Y, Bayraktar E, Mangala LS, et al. GnRH-R-targeted lytic peptide sensitizes BRCA wild-type ovarian cancer to PARP inhibition. Mol Cancer Ther 2019;18:969–79.
22. Schmittgen TD, Livak KJ. Analyzing real-time PCR data by the comparative C(T) method. Nat Protoc 2008;3:1101–8.
23. Huang J, Hu W, Hu L, Previs RA, Dalton HJ, Yang XY, et al. Dll4 inhibition plus aflibercept markedly reduces ovarian tumor growth. Mol Cancer Ther 2016;15:1344–52.
24. Love Z, Wang F, Dennis J, Awadallah A, Salem N, Lin Y, et al. Imaging of mesenchymal stem cell transplant by bioluminescence and PET. J Nucl Med 2007;48:2011–20.
25. Gao K, Li X, Zhang L, Bai L, Dong W, Gao K, et al. Transgenic expression of IL-33 activates CD8(+) T cells and NK cells and inhibits tumor growth and metastasis in mice. Cancer Lett 2013;335:463–71.
26. Gao Y, Ma L, Luo CL, Wang T, Zhang MY, Shen X, et al. IL-33 exerts neuroprotective effect in mice intracerebral hemorrhage model through suppressing inflammation/apoptotic/autophagic pathway. Mol Neurobiol 2017;54:3879–92.
27. Tilstra JS, Avery L, Menk AV, Gordon RA, Smita S, Kane LP, et al. Kidney-infiltrating T cells in murine lupus nephritis are metabolically and functionally exhausted. J Clin Invest 2018;128:4884–97.
28. Gerlach C, van Heijst JW, Swart E, Sie D, Armstrong N, Kerkhoven RM, et al. One naive T cell, multiple fates in CD8+ T cell differentiation. J Exp Med 2010;207:1235–46.
29. Millar RP. GnRHs and GnRH receptors. Anim Reprod Sci 2005;88:5–28.
30. Fost C, Duwe F, Hellriegel M, Schweyer S, Emons G, Grundker C. Targeted chemotherapy for triple-negative breast cancers via LHRH receptor. Oncol Rep 2011;25:1481–7.
31. Hislop JN, Caunt CJ, Sedgley KR, Kelly E, Mundell S, Green LD, et al. Internalization of gonadotropin-releasing hormone receptors (GnRHRs): does arrestin binding to the C-terminal tail target GnRHRs for dynamin-dependent internalization? J Mol Endocrinol 2005;35:177–89.
32. Barua S, Linton RS, Gamboa J, Banerjee I, Yarmush ML, Rege K. Lytic peptide-mediated sensitization of TRAIL-resistant prostate cancer cells to death receptor agonists. Cancer Lett 2010;293:240–53.
33. Lotzova E, Savary CA, Champlin RE. Genesis of human oncolytic natural killer cells from primitive CD34+CD33- bone marrow progenitors. J Immunol 1993;150:5263–9.
34. Kawamoto M, Horibe T, Kohno M, Kawakami K. HER2-targeted hybrid peptide that blocks HER2 tyrosine kinase disintegrates cancer cell membrane and inhibits tumor growth in vivo. Mol Cancer Ther 2013;12:384–93.
35. Hosta-Rigau L, Olmedo I, Arbiol J, Cruz LJ, Kogan MJ, Albericio F. Multifunctionalized gold nanoparticles with peptides targeted to gastrin-releasing peptide receptor of a tumor cell line. Bioconjug Chem 2010;21:1070–8.
36. Sioud M, Mobergslien A. Selective killing of cancer cells by peptide-targeted delivery of an anti-microbial peptide. Biochem Pharmacol 2012;84:1123–32.
37. Rosenberg J, Huang J. CD8(+) T cells and NK cells: parallel and complementary soldiers of immunotherapy. Curr Opin Chem Eng 2018;19:9–20.
38. Pluhar GE, Pennell CA, Olin MR. CD8(+) T cell-independent immune-mediated mechanisms of anti-tumor activity. Crit Rev Immunol 2015;35:153–72.
39. Lucarini V, Zicchedda G, Macchia I, La Sorsa V, Peschiaroli F, Buccione C, et al. IL-33 restricts tumor growth and inhibits pulmonary metastasis in melanoma-bearing mice through eosinophils. Oncoimmunology 2017;6:e1317420.

Published OnlineFirst September 17, 2020; DOI: 10.1158/1535-7163.MCT-20-0030

Molecular Cancer Therapeutics

Enhanced Immunotherapy with LHRH-R Targeted Lytic Peptide in Ovarian Cancer

Mark Seungwook Kim, Shaolin Ma, Anca Chelariu-Raicu, et al.

Mol Cancer Ther 2020;19:2396-2406. Published OnlineFirst September 17, 2020.